第41卷第1期 水电能源科学 Vol. 41 No. 1
2023年1月 Water Resources and Power Jan. 2023

DOI:10.20040/j.cnki.1000-7709.2023.20220715

输水工程无压洞与有压洞的局部水力衔接特性研究

董合费[1],徐温仁[1],赖　勇[2]

(1. 温州市瓯江引水发展有限公司,浙江 温州 325000;2. 浙江省水利水电勘测设计院有限责任公司,浙江 杭州 310002)

摘要: 无压渠道具有一定的调蓄作用,但无压变有压的衔接段局部水流相对复杂,可能形成吸气、漩涡和涌浪等不利水流现象。为研究无压隧洞下游与有压隧洞衔接段的水流形态,以温州市瓯江引水工程输水隧洞为例,根据重力相似准则搭建了30∶1的大比尺正态局部水工模型,通过观测不同工况下的过流形态、水面线分布、流速分布和波浪特性,获得了不同工况下水流的流动趋势、水深、流速和波浪特征参数。研究结果表明,通过渐变过渡的无压与有压衔接段的水流形态良好,无吸气、回流和涌浪发生,为工程的安全运行提供了支撑。

关键词: 输水工程;输水明渠;无压洞;有压洞;水流形态;模型试验

中图分类号: TV135.2　　**文献标志码:** A　　**文章编号:** 1000-7709(2023)01-0108-04

1 工程概况

温州市瓯江引水工程位于温州市区,自瓯江引水至温州城区,采用泵站提水至首部无压洞调蓄后,以有压隧洞重力流输水,总输水干线全长61 km。输水线路首段渡坪隧洞为无压洞,上游与水泵出水管路相连,下游与有压洞相连,不仅承担输水功能,且具有调蓄调压作用。因该段水流水力特性比较复杂,在与下游输水管路衔接处,水位的变化可能导致漩涡和吸气现象的发生。输水隧洞设计平均引水流量25 m^3/s,最大引水流量50 m^3/s。无压隧洞总长1.173 km,为城门洞型断面,标准洞径8.0 m×13.0 m(宽×高),最大洞径8.0 m×24.62 m(宽×高);有压输水隧洞标准洞径6.4 m×6.4 m(宽×高),在与无压隧洞连接部位顶部局部设喇叭口,见图1。目前对进水口的体型、进水池及隧洞进口的水流形态展开了大量的数值模拟和水力模型试验研究[1-3],但对于局部无压暗渠和有压隧洞直接相连的水力特性的研究相对较少。为分析无压暗渠和有压隧洞衔接段的水力特性,本文以温州市瓯江引水工程输水隧洞为例,通过大比尺的无压与有压隧洞衔接区间的水力模型试验,观测和测试了水流流态、水面线分布、水流流速分布和水面波浪过程,为瓯江引水工程渡坪段无压暗渠的安全稳定运行提供了参考依据。

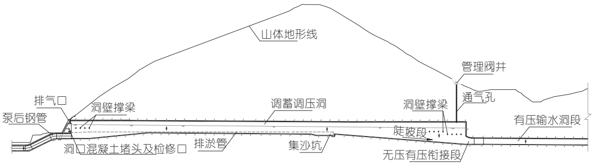

图1　无压隧洞与有压隧洞衔接布置图

Fig. 1　Layout of connection between pressureless tunnel and pressured tunnel

2 模型设计

2.1 模型相似基本原理

对于复杂的水力现象,难以通过理论分析和计算进行研究和分析。通常采用模型试验对其进行模拟和分析。渡坪隧洞下游衔接段水力学模型采用整体正态模拟,考虑到重力对渡坪隧洞中水流起主导作用,模型采用重力相似准则(弗劳德相似准则)设计。相似准则关系可表示为:

$$Fr = v/\sqrt{gL} \tag{1}$$

式中,Fr 为弗劳德数;v 为流速;g 为重力加速度;L 为特征长度。

2.2 模型范围和比尺计算

根据渡坪隧洞的具体情况,试验模型建造范围为无压有压衔接处上游约200 m,无压隧洞下游隧洞约100 m,试验模拟原型范围约为300 m×10 m×25 m(长×宽×高)。结合试验场地、供水能力,确定模型的几何比尺为30∶1,模型尺

收稿日期: 2022-03-11,**修回日期:** 2022-04-25
基金项目: 浙江省水利厅科技项目(RA2011)
作者简介: 董合费(1976-),男,硕士、高级工程师,研究方向为工程水力学、水工结构,E-mail:327752391@qq.com

寸为 10 m×0.4 m×0.9 m(长×宽×高)。基于模型比尺、重力设计准则计算模型的相似比尺见表 1。

表 1　无压渐变有压隧洞模型比尺计算表

Tab. 1　Model scale calculation of gradual change from non pressure tunnel to pressure tunnel

参数	计算依据	比尺	原型	模型
几何比尺	λ_L	30.00	30 m	1 m
流速比尺	$\lambda_V=\lambda_L^{1/2}$	5.48	32.00 m/s	5.84 m/s
流量比尺	$\lambda_D=\lambda_L^{5/2}$	4 929.50	50.00 m^3/s	0.010 m^3/s
时间比尺	$\lambda_T=\lambda_L^{1/2}$	5.48	1.00 s	0.18 s
重度比尺	$\lambda_\gamma=\lambda_G/\lambda_V$	1	9 800 N/m^3	9 800 N/m^3
粗糙比尺	$\lambda_n=\lambda_L^{1/6}$	1.76	0.014 0	0.007 9

根据模型比尺，由于混凝土糙率接近 0.014，要求模型材料的糙率约为 0.007 9，有机玻璃的糙率约为 $n=0.008\ 0$，与之最为接近，故模型选用有机玻璃。

2.3　工况选取

在平均流量、最大流量供水规模 $Q=25$、50 m^3/s 情况下，试验对渡垟隧洞下游进行了流态观测，对沿程水面线、沿程流速分布、有压无压衔接段的波浪特性进行测量，相关工况见表 2。

表 2　供水流量 $Q=25$、50 m^3/s 工况衔接处水位

Tab. 2　Water supply flow $Q=25$、50 m^3/s working condition

工况	上游流量	下游流量	衔接处水位/m	工况	上游流量	下游流量	衔接处水位/m
GS01	25.0	25.0	18.965	GM01	50.0	50.0	28.300(典型工况)
GS02	25.0	25.0	19.465	GM02	50.0	50.0	27.800
GS03	25.0	25.0	20.000(典型工况)	GM03	50.0	50.0	27.300
GS04	25.0	25.0	20.465	GM04	50.0	50.0	26.800
GS05	25.0	25.0	20.965	GM05	50.0	50.0	26.300
GS06	25.0	25.0	21.465	GM06	50.0	50.0	25.800

注：上游流量、下游流量单位均为 m^3/s。

3　试验测试

3.1　流态分析

试验对各工况下无压输水洞段、衔接段、有压隧洞段的水流流态进行了观测分析。试验过程观察憋气和脱壁现象并录制视频，未发现憋气和脱壁现象，对于负压问题，在过水断面变化点装置了测压管，这些测压管和大气连通，试验过程中通过观测是否有气体吸入来判断该处是否有负压发生。典型工况 GM01 和 GS03 的试验观测结果均表明，在无压输水洞段区间，水面平静，分布均衡，水流顺直平稳，无明显波动和偏流现象发生；在有压与无压衔接段，水流横向平缓过渡，无收缩导致的脱壁和回流现象发生，水流纵向由深水渐变至有压洞顶部，水流变化平缓，无脱壁和吸气现象发生，进口上游水面未观测到旋涡和回流现象。在有压隧洞区间，水流进入有压隧洞段后，无憋气、脱壁和负压等不利水流现象发生，整体流态良好。

3.2　渡垟隧洞下游衔接段水面线测试

为分析渡垟隧洞下游与有压洞衔接区间的水面特性，在不同供水规模情况下，测量了渡垟隧洞下游沿程水面线，分别测量了 10 个测量断面的两壁与中间点的水位，水位测点共计 30 个。典型工况 GM01 和 GS01 的水面线观测结果见表 3，水面线见图 2。试验结果表明，渡垟隧洞下游衔接段底坡为顺坡，且坡度大于临界坡度，即 $i=8\%>i_c=0.16\%>0$，属于陡坡渠道，临界水深大于正常水深。同时因渠道沿程水深均大于临界水深，即 $h>h_c$，该区的纵向水面线分布属于 s1 型壅水曲线，水深沿程增加。区间整体水面平静，水面纵向水平分布，水面横向分布均衡。

表 3　最大流量工况 GM01 和平均流量工况 GS01 水面线分布

Tab. 3　Water surface profile distribution of GM01 under maximum flow condition and GS01 under average flow condition

m

工况	断面	桩号	左壁面	中心点	右壁面
最大流量工况 GM01	1	DY0+982.50	28.327	28.323	28.313
	2	DY1+004.10	28.300	28.292	28.323
	3	DY1+029.00	28.306	28.294	28.335
	4	DY1+049.40	28.317	28.315	28.324
	5	DY1+070.70	28.309	28.335	28.298
	6	DY1+092.30	28.338	28.292	28.299
	7	DY1+117.20	28.317	28.298	28.323
	8	DY1+138.80	28.298	28.307	28.315
	9	DY1+160.37	28.333	28.291	28.299
	10	DY1+170.75	28.302	28.306	28.315
平均流量工况 GS01	1	DY0+982.50	20.013	19.997	19.984
	2	DY1+004.10	20.015	19.981	20.003
	3	DY1+029.00	20.010	20.007	20.015
	4	DY1+049.40	20.019	19.995	20.007
	5	DY1+070.70	20.018	19.995	19.984
	6	DY1+092.30	19.995	20.028	20.003
	7	DY1+117.20	20.026	20.005	20.018
	8	DY1+138.80	20.029	20.002	19.981
	9	DY1+160.37	19.994	19.986	20.021
	10	DY1+170.75	20.054	19.980	20.098

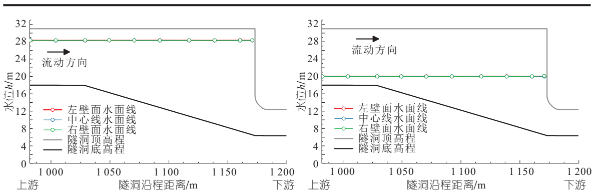

(a) 最大流量工况GM01　　(b) 平均流量工况GS01

图 2　衔接段沿程水面线分布图

Fig. 2　Distribution of water surface line along the connecting section

3.3　下游衔接段流速分布测试

在不同供水规模情况下,测量了渡坪隧洞下游沿程流速分布。从桩号 DY0＋982.50 至 DY1＋170.75 之间共取 10 个测量断面,每个测量截面上 3 个测点,分别为截面中心的水面位置、水面下 1.5、4.5 m 处,典型工况的流速测试结果见表 4、图 3。试验结果表明,衔接段区间属 s2 型壅水曲线,水深沿程增加,断面平均水流流速沿程减小。同时由于衔接段开口位于边壁底部,则在靠近衔接段处水位越深,流速越大。

表 4　最大流量工况和平均流量工程衔接段沿程流速分布

Tab. 4　Velocity distribution along connecting section of the maximum flow connection section and average flow condition

m/s

工况	断面	桩号	水面位	水面下 1.5 m	水面下 4.5 m
最大流量	1	DY0＋982.50	0.619	0.378	0.378
	2	DY1＋004.10	0.674	0.559	0.499
	3	DY1＋029.00	0.855	0.815	0.734
	4	DY1＋049.40	0.832	0.674	0.411
	5	DY1＋070.70	0.526	0.471	0.438
	6	DY1＋092.30	0.499	0.378	0.351
	7	DY1＋117.20	0.378	0.411	0.411
	8	DY1＋138.80	0.378	0.290	0.351
	9	DY1＋160.37	0.142	0.263	0.263
	10	DY1＋170.75	0.082	0.155	0.323
平均流量	1	DY0＋982.50	2.114	/	/
	2	DY1＋004.10	2.126	/	/
	3	DY1＋029.00	2.154	1.830	/
	4	DY1＋049.40	1.595	1.030	/
	5	DY1＋070.70	1.211	0.882	0.230
	6	DY1＋092.30	0.619	0.499	0.411
	7	DY1＋117.20	0.526	0.471	0.471
	8	DY1＋138.80	0.378	0.499	0.351
	9	DY1＋160.37	0.142	0.290	0.290
	10	DY1＋170.75	0.142	0.203	0.323

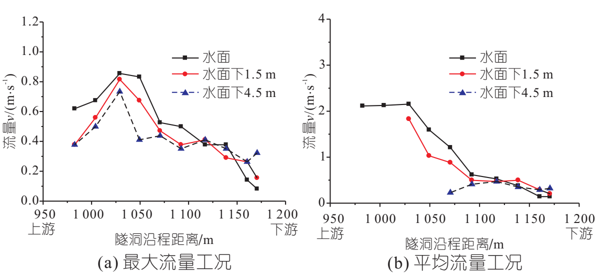

图 3　衔接段沿程流速分布图

Fig. 3　Flow velocity distribution along the connecting section

3.4　衔接段波浪测试

在不同供水规模情况下,采用波高仪动态观测了渡坪隧洞下游衔接段的水位波动。波浪测点共计 3 个,在桩号 DY1＋170.75 的 10 号断面处从左到右均匀分布,典型工况波浪测试结果见表 5、图 4。波浪测试结果表明,衔接段最大浪高为 0.265 m,最大水面高程为 28.357 m,隧洞具有一定的安全超高和富裕高度,无水流触顶现象。

表 5　最大流量工况和平均流量工况衔接段波浪特征值

Tab. 5　Wave characteristic value of connecting section under maximum flow condition and average flow condition

m

工况	测点位置	平均值 $\bar{h}$	最大值 h_{max}	最小值 h_{min}	浪高 Δh
最大流量	右	28.302	28.327	28.276	0.051
	中	28.312	28.357	28.267	0.091
	左	28.300	28.332	28.267	0.065
平均流量	右	19.982	20.057	19.907	0.150
	中	20.011	20.083	19.939	0.144
	左	19.991	20.081	19.901	0.180

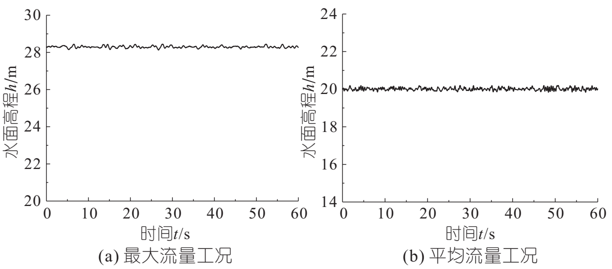

图 4　衔接段水面波动时程线

Fig. 4　Time history of water surface fluctuation in connecting section

4　结论

a. 通过在隧洞进口上部采用椭圆形曲线,两侧采用渐缩性体型,可有效防止旋涡和脱壁现象。在无压输水洞段区间,水面平静、分布均衡、水流顺直平稳,无较明显波动和偏流现象发生,不会发生水流触顶现象。

b. 在有压与无压衔接段,水流横向平缓过渡,无收缩导致的脱壁和回流现象发生,水流纵向由深水渐变至有压洞顶部,水流变化平缓、无脱壁和吸气现象发生,进口上游水面未观测到旋涡和回流现象。

c. 在有压隧洞区间,水流进入有压隧洞段后,无憋气、脱壁和负压等不利水流现象发生,整体流态良好。

参考文献:

[1]　陈桂友, 赵青, 穆仁会. 引水隧洞进口明满流数值模拟[J]. 南水北调与水利科技, 2016,14(4):163-167,209.

[2]　李伟, 王韦, 田忠, 等. 折流坎高度对导流洞交汇段水力特性的影响[J]. 水电能源科学, 2019,37(7):78-80, 85.

[3]　梁文龙, 李贵平, 余跃. 隧洞进水口及洞内消能水工模型试验研究[J]. 贵州工业大学学报(自然科学版), 2001(3):95-100.

Study on Hydraulic Connection Characteristics of Local Open Channel and Pressurized Tunnels in Water Transfer Project

DONG He-fei[1], XU Wen-ren[1], LAI Yong[2]

(1. Wenzhou Oujiang Water Diversion Development Limited Company, Wenzhou 325000, China;
2. Zhejiang Design Institute of Water Conservancy and Hydro-electric Power Co., Ltd., Hangzhou 310002, China)

Abstract: The local open channels play a certain role in regulating and storing water, but the water flow in the junction section with open channel variation and pressure is relatively complex, which may cause adverse water flow phenomena such as air intake, whirlpool and surges. In order to study the hydraulic pattern of the connecting section between the open channel and the pressurized tunnel, based on the water conveyance tunnel of Wenzhou Oujiang water diversion project, a 30:1 large scale normal local hydraulic model was built according to the gravity similarity criterion. The hydraulic pattern, water surface line distribution, velocity distribution and wave characteristics under different conditions were observed through hydraulic model tests. The flow trend, depth, velocity and wave characteristic parameters under different working conditions were obtained. The research results show that the flow in the open channel and the pressurized junction section through the gradual transition is in good shape, and there is no air intake, backflow and surge, which provides support for the safe operation of the project.

Key words: water transfer project; open channel flow; free water tunnel; pressurized tunnel; hydraulic pattern; model test

(上接第 154 页)

Effect of Coplanar Double Fissures on Mechanical Properties and Failure Characteristics of Sandstone

ZHANG De-chao, XIAO Tao-li, SHE Hai-cheng

(School of Urban Construction, Yangtze University, Jingzhou 434023, China)

Abstract: The internal defects of rock mass have a significant effect on its mechanical properties and damage and fracture. The influence of fissure angles and bridge lengths on rock mechanical properties and failure was analyzed by uniaxial compression test and DIC technique. The research findings are as follows: The peak stress and elastic modulus of the samples have an obvious change trend with the change of the fissure angle. Compared with the length of the rock bridge, the fissure angle has a more significant effect on the mechanical properties of the rock. With the increase of fissure angle, the number of surface cracks, main failure cracks and surface spalling decreases, while the area of falling blocks increases obviously. However, with the increase of bridge length, the characteristics of crack propagation and spalling are basically the same. In the process of crack propagation, the connection of rock bridge is related to the fissure angle and the length of rock bridge. In the low fissure angle, the failure mode of rock samples is dominated by tensile failure cracks; With the increase of the fissure angle, the performance is as follows: the tension damage crack to shear damage crack transformation to form a mixed tensile shear damage mode; At the same time, with the increase of bridge length, the more difficult the rock bridge is to penetrate, and the local crack expansion failure changes from tensile-shear crack to tensile crack.

Key words: sandstone-like; coplanar double fissures; fissure angle; rock bridge length; DIC technique

(上接第 158 页)

Effect of Temperature and Salinity on Shear Mechanical Properties of Coral Sand

LI Bei[1], LEI Xiao[2], XU Jia-peng[1], GUO Yu[1], XU Xiao-liang[1]

(1. Laboratory of Geological Hazards on Three Gorges Reservoir Area, Ministry of Education, China Three Gorges University, Yichang 443002, China; 2. Power China Sichuan Electric Power Engineering Co., Ltd., Chengdu 610000, China)

Abstract: Coral sand is an important material for island and reef engineering construction. Its physical and mechanical properties in different marine environments directly affect the design, construction and long-term operation of island and reef structures. In order to study the shear mechanical properties of coral sand under the influence of temperature and salinity, the triaxial drainage shear tests of coral sand in the South China Sea were carried out at different temperatures and salinity by using the self-developed temperature controlled pile-soil interface triaxial tester. The results show that similar to ISO standard sand, the shear stress-strain curves of coral sand have peaks, presenting its characteristics of strain softening; The shear strength of coral sand is not significantly affected by temperature, but it is sensitive to salinity. Compared with fresh water environment, the peak shear strength of coral sand in salt water environment decreases by 2.5%-8.5%, and the lower of confining pressure, the greater of decrease range; Salinity has a deterioration effect on the cohesion of coral sand, and its reduction range is about 30%, but the effect on the internal friction angle of coral sand is not obvious.

Key words: coral sand; shear strength; temperature; salinity; cohesion